ASME 2012 5th Annual Dynamic Systems and Control Conference joint with the JSME 2012 11th Motion and Vibration Conference
DSCC2012-MOVIC2012
October 17-19, 2012, Fort Lauderdale, Florida, USA

DSCC2012-MOVIC2012-8775

INTEGRATED TRAJECTORY PLANNING, SYSTEM MODELING, AND CONTROL DESIGN FOR OPTIMIZED MOTOR SELECTION

Aderiano da Silva
Dept. of Mechanical Engineering
Marquette University
Milwaukee, WI 53201
aderiano.dasilva@marquette.edu

Philip A. Voglewede
Dept. of Mechanical Engineering
Marquette University
Milwaukee, WI 53201
philip.voglewede@marquette.edu

Kevin C. Craig
Dept. of Mechanical Engineering
Marquette University
Milwaukee, WI 53201
kevin.craig@marquette.edu

ABSTRACT

In addition to a well-designed and tuned control system and a properly designed mechanical system, accurate motion control in industrial machines heavily depends on trajectory planning and the appropriate selection of the motors controlling the axes of the machine. A model-based design approach to properly select a motor prior to building a prototype is proposed in this paper. Additionally, a trajectory planning approach is proposed and demonstrated to improve position control accuracy of industrial machines. The proposed motor selection process and trajectory planning approach are demonstrated via modeling and simulation of a commonly used planar robot (H-Bot).

INTRODUCTION

Model-based design has been of fundamental importance for industrial development during the past few decades [1-8]. It has gained even more interest from the scientific and industrial communities, as the needs for energy efficiency, reliability, flexibility, and accuracy have increased to satisfy a market that is demanding higher productivity at reduced costs in a sustainable manner. Tighter, more complex, and challenging specifications need to be achieved [1, 2]. As machines become more complex, model-based design has helped engineers overcome the challenges in mechatronic system design [1,3-8]. In a mechatronic system design approach, many stages of the design process overlap and all disciplines including mechanical, electrical, and computer systems are fully integrated to enhance the synergy among them. This is leveraged by virtual prototyping and modeling that allows the integration, evaluation, and simulation of various scenarios before a system is built.

A critical issue that machine builders face in the design stage is the selection of motors, gearing systems, and electronics to control each axis of a machine. To overcome this challenge, a model-based design approach to properly select motors for a machine prior to building a prototype is presented in this paper. In this approach, the inverse kinematics of the system, in conjunction with trajectory planning, is used to compute the motion profiles of the motors. These motion profiles feed the inverse kinetic model of the system that is simulated in open loop to compute the required motor torque vs. speed curves. These are used to select candidate motors. After selecting candidate motors, the inertia and losses of the motor and gear system are included in a closed-loop simulation to validate the solution and stability of the system. This approach allows simulating not only the mechanical system, but also the control scheme of the system in an integrated manner. This approach can also help uncover issues before building the prototype, in addition to closing the gap between the mechanical and control designs.

The proposed motor selection process is demonstrated in this paper by selecting the motors for a planar robot called an H-Bot, which consists of two motors, a timing belt, and two rails mounted perpendicular to each other. The physical system of this robot is shown in Fig. 1. An H-bot is a two-dimensional robot extensively used in industry in applications such as pick-and-place, sorting, gluing, and inspection. This type of robot is particularly attractive for machine builders due to the relatively ease of manufacturing. Although this motor selection process will be demonstrated with a robot, it is a generic method that can be applied to any industrial machine.

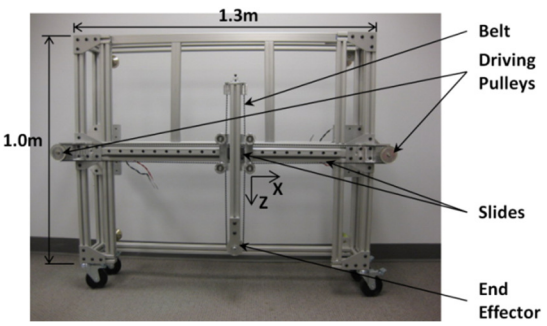

FIGURE 1. PHYSICAL SYSTEM OF AN H-BOT.

An appropriated motion profile is not only critical for the motor selection process, but also for the overall performance of the system. However, motion systems often use jerky motion profiles that stress the machine and motors, and produce unwanted vibrations and wear, which result in poor performance and shortened life [9-12]. This is due to the use of inappropriate motion profiles or poor trajectory planning. A typical type of motion profile is the trapezoidal profile, which consists of an acceleration segment, a constant-speed segment and a deceleration segment. Theoretically, infinite jerk occurs at the beginning and end of the acceleration and deceleration segments of a trapezoidal profile. This type of profile is often used because industrial controllers used to program machines provide readily available and easy-to-use tools to build simple motion profiles, such as trapezoidal profiles. Meanwhile, the process of building a more complex and efficient profile is more involved, requiring more programming and knowledge. This results in an easy choice for the less-efficient motion profiles. Additionally, some types of trajectories are particularly difficult to accurately follow, e.g. square shapes. This can yield large positioning error even if a well-tuned control scheme is used with a well-designed mechanical system. The difficulty with square shapes resides in accurately tracing the corners, which can result in imperfections to the actual product. This issue is mitigated by trajectory planning, which is a method to calculate the position reference for each axis of a mechanism in such a way that position-following error and jerk are reduced. A trajectory planning approach to mitigate undesirable positioning errors is described in this paper and demonstrated with simulation results.

In the next section, the proposed motor selection process and a trajectory planning approach are presented. This is followed by simulation results and conclusions.

PROPOSED MOTOR SELECTION PROCESS

The proposed motor selection process employs model-based design to improve the process of choosing motors for motion applications. Since this method allows selecting the motor while in the design stage of the system, trial-and-error tests and physical prototyping are avoided. This reduces the design costs and allows faster delivery of the system.

Each step of this proposed motor selection process is shown in Fig. 2. These steps are described and demonstrated next by selecting the motors for an H-bot tracing a square shape.

System requirements

The system requirements define the minimum functionalities and indices of performance that the system needs to achieve. This may include the envelope of motion, trajectory, maximum positioning accuracy, machine cycle time, pay load, and maximum allowable level of vibration and noise. The system requirements are, in general, contained in the functional specifications of the machine. For the H-Bot, the system requirements consist of performing the square shape shown in Fig. 3 with diagonal of 0.4 meters in 2 seconds with a maximum position error of 1mm.

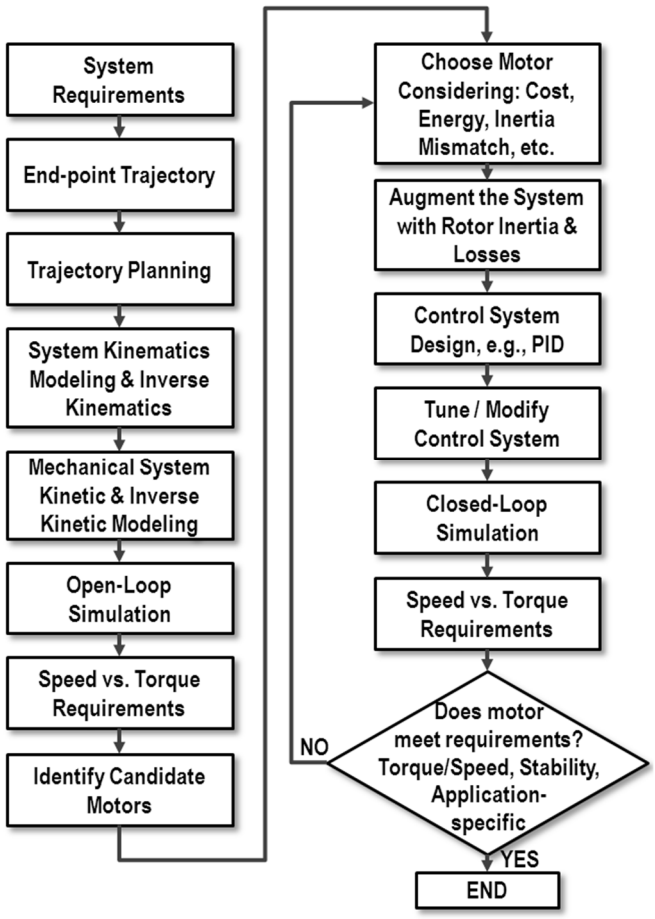

FIGURE 2. PROPOSED MOTOR SELECTION PROCESS

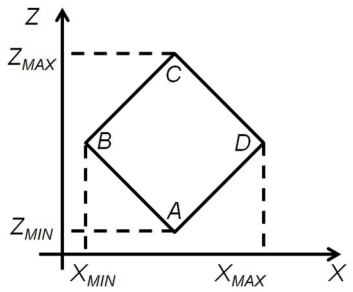

FIGURE 3. DEFINITIONS TO THE SQUARE SHAPE

End-Point trajectory

The end-point trajectory is defined here as the motion of the end-effector. Depending on the type of mechanism, the end-point trajectory can be defined in reference to different points on a machine, e.g., at the end-effector for robots, at the platen for presses, and at the load for conveyors. The end-point or end-effector trajectory is defined for the worst-case trajectory that the end-effector must perform. This worst-case trajectory is identified from the functional specifications of the machine. The worst-case trajectory is, in general, defined as a function of the application requirements and not in terms of the maximum capability of the mechanism. This may allow selecting smaller

motor sizes. It is essential to define the end-point trajectory first, because the required torque vs. speed curve used to size the motor depends on it.

If the system needs to perform multiple types of trajectories, designing motors and drives for the worst case is enough. If it is not obvious which trajectory is the worst case, either all, or the most likely worst cases, must be evaluated to identify which one requires the greatest motor and drive utilization. When the mechanism can perform an infinite number of different trajectories, such as a pick-and-place mechanism with a vision system to locate products in random orientation and location, the boundary conditions of the worst-case trajectory need to be determined in order to estimate the worst-case trajectory to be used in the motor selection process.

For this case-study of an H-Bot, the square path with a diagonal of 0.4 meters, traced in 2 seconds, was identified from the functional specification of the machine as the worst case trajectory for this particular system.

Trajectory Planning

Trajectory planning is the computation of motion profiles for the actuators of automatic machines, e.g., packaging machines, machine tools, assembly machines, metal-forming machines, and industrial robots. Such motion profiles need to be defined in a way to avoid or reduce the amount of mechanical vibration, stress on mechanical and electronic components, electrical and audible noise, stress on motors and actuators, as well as to reduce overshoot response and excessive position error during motion.

The information necessary to compute the trajectory planning is the end-point trajectory and inverse kinematics of the mechanism. Since kinetic models are not necessary at this point, the trajectory planning can be defined at the early stages of the design from sketches with the main dimensions of the moving mechanism. Thus, there is no need for information about masses and mass moments of inertia of the system for trajectory planning.

Trajectory planning is particularly important to reduce position tracking errors in machines such as machine tools while performing certain types of profiles [13]. This includes profiles with sharp corners in coordinated motion systems. A typical example of such a profile is a square shape. The difficulty with square shapes resides in accurately tracing the corners without overshoots or distortions that can cause imperfections to the final product.

A trajectory planning approach that can be applied to general types of industrial machines is given next. This approach is demonstrated with an H-Bot tracing a square shape. After defining the end-point trajectory, this approach consists of the following steps.

Identify points in the end-point trajectory in which the velocity changes direction. These are the points in which at least one axis from the same coordinated motion system changes the direction of motion. In the case of the square shape, shown in Fig. 3, this occurs at the corners. In corners A and C, the Z axis changes direction, while in corners B and D, the X axis changes direction.

Define the master command. The master command or master reference is used to synchronize the motion of the axes in the system. In industrial applications, this master reference is, in general, a virtual axis, i.e., an axis that only exists in the machine code without any hardware (e.g., drives, motors) associated with it. Its purpose is the synchronization of the physical axes via a common reference command. The master reference needs to be defined as a profile that helps reduce vibration, mechanical and electrical stresses, and noise on the physical axes. However, the master reference is in general set to constant speed which can yield trapezoidal profiles on the physical axes for certain types of end-point trajectories, and consequently cause these undesirable effects [14, 15]. Thus, the master reference needs to be defined as a motion profile that mitigates these effects. Motion profiles with zero acceleration at the beginning and end of the move yield smoother motion for physical systems. Although various types of profiles could be used to build the master reference, the 5th-order polynomial profile [14] yields a good tradeoff between smoothness and peak velocity. The master reference will consist of segments located between every two consecutive points of the end-effector trajectory that has a change in polarity on the velocity profile. Thus, the master position command (S_M) can be defined for each one of these segments as a 5th-order polynomial profile as follows:

$$S_M = 10\left(\frac{t}{T}\right)^3 - 15\left(\frac{t}{T}\right)^4 + 6\left(\frac{t}{T}\right)^5 \qquad (1)$$

T is the desired time to complete each segment and t is the instantaneous time. The master command for the H-Bot contains four segments ($\overline{AB}, \overline{BC}, \overline{CD}, \overline{DA}$) located between each corner of the square shape as shown in Fig. 4. The master position command has unitary increment from segment to segment. This unitary increment continues until it completes the entire end-point trajectory. Then the master command can either continue the unitary increment into the next machine cycle or be reset back to zero. The duration of each segment is given by T. The desired time T depends on the time to perform each segment, which may not be the same for all segments.

In the design of a single-axis system, Eq. (1) can be used directly to define the command position of the motor. In case of coordinated systems (resulting motion depends on two or more axes, such as in an H-Bot), Eq. (1) defines the master command that in used with the geometric equations to calculate the command position of the motors, as described next.

Identify geometric equations. The geometric equations describe the end-point trajectory as coordinates in the Cartesian space. The number of geometric equations is given by the degree

of freedom of the end-point trajectory. In the H-Bot case, the end-point trajectory is in the XZ plane. Thus, there are two geometric equations, one to describe the motion in *X* and one in *Z*. The geometric equations of the H-Bot performing the square shape shown in Fig. 3 are as follows:

$$X = \begin{cases} ((X_{MAX} - X_{MIN})/2)(1 - S_M) + X_{MIN} & \overline{AB} \\ ((X_{MAX} - X_{MIN})/2)(-1 + S_M) + X_{MIN} & \overline{BC} \\ ((X_{MAX} - X_{MIN})/2)(-1 + S_M) + X_{MIN} & \overline{CD} \\ ((X_{MAX} - X_{MIN})/2)(5 - S_M) + X_{MIN} & \overline{DA} \end{cases}$$
$$Z = \begin{cases} ((Z_{MAX} - Z_{MIN})/2)S_M + Z_{MIN} & \overline{AB}, \overline{BC} \\ ((Z_{MAX} - Z_{MIN})/2)(4 - S_M) + Z_{MIN} & \overline{CD}, \overline{DA} \end{cases} \quad (2)$$

X_{MAX}, X_{MIN}, Z_{MAX} and Z_{MIN} are the maximum and minimum displacements in the *X* and *Z* directions, respectively. The resulting profiles for *X* and *Z* obtained from Eq. (2), with X_{MIN} and Z_{MIN} equal to zero and the master command (S_M) defined in Eq. (1) for the H-Bot tracing a square shape with diagonal of 0.4 meters in 2 seconds, is shown in Fig. 5.

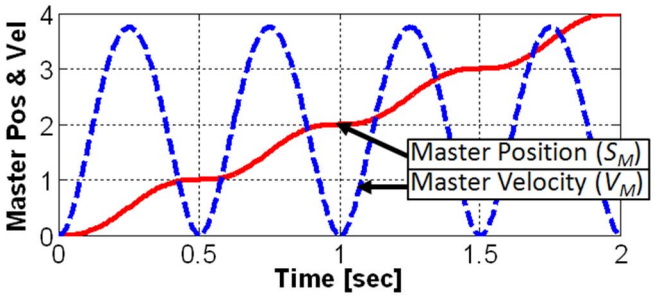

FIGURE 4. MASTER COMMAND FOR H-BOT.

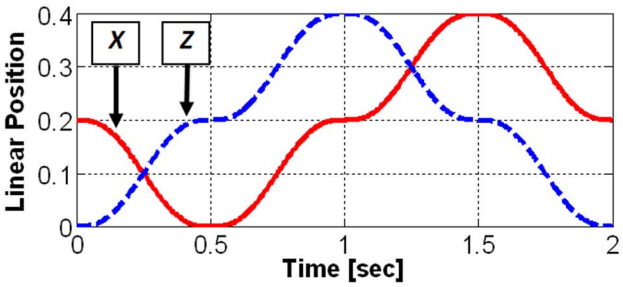

FIGURE 5. SQUARE PROFILE SPLIT IN X AND Z AXES ACCORDING TO PRESENTED TRAJECTORY PLANNING.

For comparison purposes, if the master command is set to a constant speed, as in traditional trajectory-planning approaches, the resulting profiles for *X* and *Y* are triangular, as shown in Fig. 6. Consequently, high acceleration is present at every 0.5 seconds which yields high acceleration torque that is proportional to inertia and acceleration. This effect is shown later in the simulation results. Smother motion profiles would be obtained by employing the presented trajectory planning method.

The values of *X* and *Z* defined in Eq. (2) from the master command S_M defined in Eq. (1) can then be applied to the inverse kinematics of the system to compute the motor motion profiles, as described next.

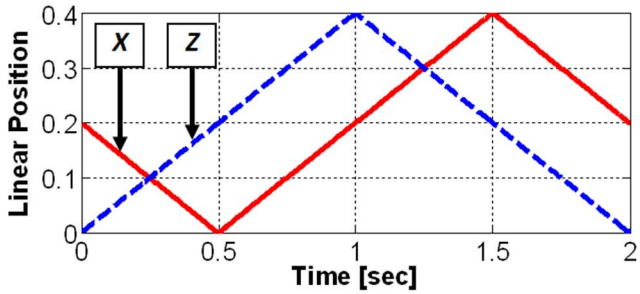

FIGURE 6. SQUARE PROFILE SPLIT IN X AND Z AXES FOR A CONSTANT SPEED MASTER COMMAND.

Inverse kinematics

The inverse kinematics (geometry of motion) of the mechanism converts the end-point trajectory described in the Cartesian space into the motion profiles that control the motors. In the case of a mechanism with redundant degrees of freedom, e.g., a 7-degree-of-freedom manipulator, infinite possibilities of motion profiles of the motors can be defined to yield the same end-point trajectory [16, 17]. In this case, one of the possible inverse kinematic solutions needs to be chosen [17] to perform the motor selection. The inverse kinematics of the case-study H-Bot is given next.

The diagram of an H-Bot is shown in Fig. 7 and it works as follows. If one motor stays stationary and the other one rotates, the end effector moves diagonally. If both motors rotate at the same speed in the same direction, the end effector moves left or right. If both motors spin at the same speed in opposite directions, the end effector moves up or down. Accordingly, the inverse kinematics of this type of robot can be derived and results in Eq. (3).

$$\theta_A = \frac{Z - X}{r}$$
$$\theta_B = \frac{-Z - X}{r} \quad (3)$$

θ_A is the angular position of motor shaft A, θ_B is the angular position of motor shaft B, *X* and *Z* define the position of the end effector in the Cartesian space given by the trajectory planning in Eq. (2), and *r* is the radius of the driving pulley connected to each motor as shown in Fig. 7. The resulting profile from the inverse kinematics in Eq. (3) with *X* and *Z* computed from the trajectory planning defined in Eq. (1) and (2) is shown in Fig. 8.

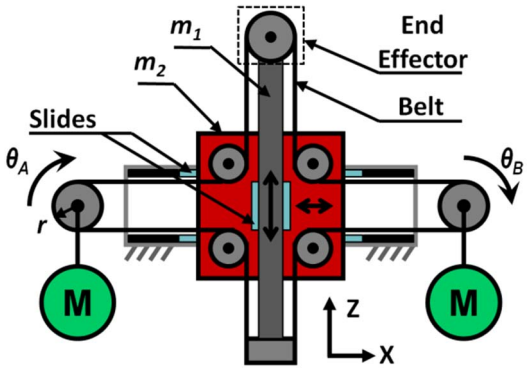

FIGURE 7. DIAGRAM OF AN H-BOT.

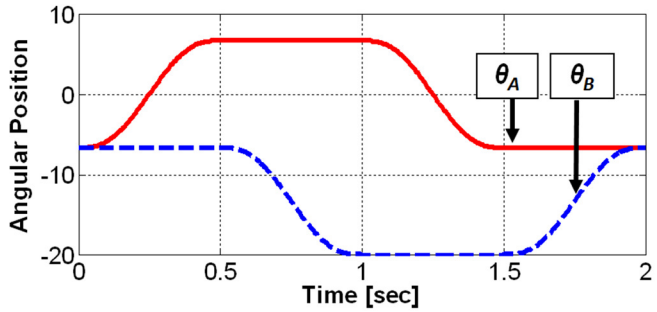

FIGURE 8. PROFILE FOR θ_A AND θ_B OBTAINED FROM THE INVERSE KINEMATICS OF THE H-BOT

Kinetic Model and Inverse Kinetic Model

The inverse kinetic model (geometry plus all torques and mass moments of inertia) is used to compute the torque that each motor needs to apply to the system to follow the required motor motion profile given by the inverse kinematics. Thus, the input of the inverse kinetic model is the motor angular position profile while the output is the motor torque. The inverse kinetic model is obtained from the kinetic model that can be derived by methods such as Newton-Euler and Lagrange. Alternatively, SimMechanics™ from MathWorks can be used to develop the kinetic model of the system [18]. If the mechanism was designed in a 3D Software package, it may be possible to automatically generate the SimMechanics model via SimMechanicsLink.

The kinetic model of the H-Bot was developed with the following assumptions: vertically mounted, massless belt, rigid bodies, frictionless joints, and inertialess idler-pulleys. By employing the Lagrange's method [19], the equations of motion are obtained. Lagrange's Equations are as follows:

$$\frac{d}{dt}\left(\frac{\partial T}{\partial \dot{q}_i}\right)-\frac{\partial T}{\partial q_i}+\frac{\partial V}{\partial q_i}=Q_i, \tag{4}$$

where, T is kinetic energy, V is the potential energy, and Q_i are the generalized forces/ torques for each generalized coordinate, q_i. The generalized coordinates are $q_1 = \theta_A$ and $q_2 = \theta_B$. The kinetic energy (T) of the system is $T = T_1 + T_2 + T_A + T_B$, while the potential energy (U) is $U = U_1 + U_2 + U_A + U_B$ with $U_2 = U_A = U_B = 0$. T_1, T_2, T_A, T_B and U_1, U_2, U_A, U_B are the kinetic energy and potential energy of body 1 (vertical moving element), body 2 (horizontal moving element), driving pulley A and driving pulley B, respectively (see Fig. 7). For this particular case:

$$T=\frac{1}{4}r^2m_1\left(\dot{\theta}_A^2+\dot{\theta}_B^2\right)+\frac{1}{8}r^2m_2\left(\dot{\theta}_A^2+\dot{\theta}_B^2+2\dot{\theta}_A\dot{\theta}_B\right)+\frac{1}{2}I_A\dot{\theta}_A^2+\frac{1}{2}I_B\dot{\theta}_B^2$$
$$U=\frac{1}{2}rm_1g\left(\theta_A-\theta_B\right) \tag{5}$$

The generalized torques are $Q_1 = \tau_A$ and $Q_2 = \tau_B$. Thus, applying Lagrange's Equations to T, U and Q_i, the following equations of motion are obtained:

$$\ddot{\theta}_A\frac{r^2}{4}\left(2m_1+m_2+\frac{4}{r^2}I_A\right)+\ddot{\theta}_B\frac{r^2}{4}m_2+\frac{1}{2}rm_1g=\tau_A$$
$$\ddot{\theta}_B\frac{r^2}{4}\left(2m_1+m_2+\frac{4}{r^2}I_B\right)+\ddot{\theta}_A\frac{r^2}{4}m_2-\frac{1}{2}rm_1g=\tau_B \tag{6}$$

$\ddot{\theta}_A$ and $\ddot{\theta}_B$ are the angular accelerations of the driving pulleys, I_A and I_B are the inertias of the driving pulleys, r is the radius of each driving pulley, m_1 is the mass of the vertical moving element, m_2 is the mass of the horizontal moving element, τ_A and τ_B are the motor torques, and g is the acceleration of gravity (see Fig. 7). The inverse kinetic model obtained from these equations was implemented in Simulink as shown in Fig. 9. The motor command positions θ_A and θ_B were obtained from the inverse kinematics defined in Eq. (3). For higher fidelity of the results, more complete equations of motion can be derived by including effects such as belt stiffness, idler-pulley inertia, and friction. The load mass and any external forces / torques can be added to the equations of motion at this point. The level of complexity included in the model of a mechanism is in general associated with the risk of the design. The risk can be measured in terms of the experience with similar mechanisms, importance to the overall process or machine, amount of innovation in the design, safety concerns, etc. High risk designs require more complete and accurate models. In this particular case-study, the model in Eq. (6) was considered enough for the sake of simplifications in this paper.

Open-Loop Simulation

The open-loop simulation is used to estimate the torque vs. speed curves that will be required from the motors to drive the system through the end-point trajectory. The model for this simulation consists of the motion profile obtained from inverse kinematics and trajectory planning applied to the inverse kinetic model of the system, as shown in Fig. 10. The kinetic model and

the additional summation blocks in this figure, although not always necessary, can help reduce the position error and more accurately estimate the motor torque. The position error (e_A and e_B) can be estimated, as shown in Fig. 10, by comparing the error between the reference signal and the motor position from the kinetic model.

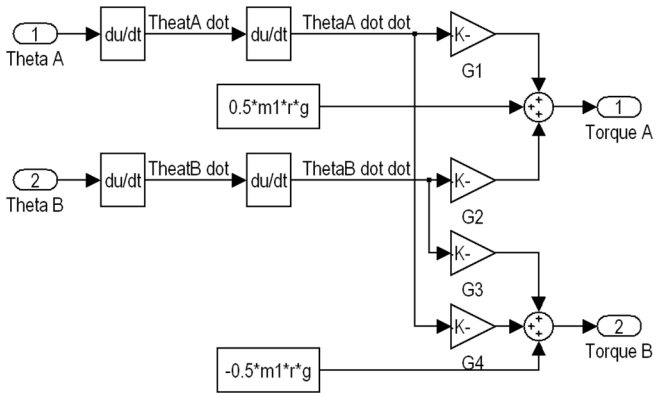

FIGURE 9. INVERSE KINETIC MODEL OF THE H-BOT WHERE G1= $(r^2/4)[2m_1+m_2+(4I_A/r^2)]$, G2= $r^2m_2/4$; G3= $(r^2/4)[2m_1+m_2+(4I_B/r^2)]$; AND G4= $r^2m_2/4$

The Simulink model to perform the open-loop simulation of the mechanism of the H-Bot is shown in Fig. 10. The "H-Bot Position Reference" block consists of equations Eq. (1), (2), and (3) from the trajectory planning and inverse kinematics. The motion profile obtained from this block is shown in Fig. 8. Meanwhile, the block called "H-Bot Inverse Kinetic" contains the inverse kinetic model shown in Fig. 9.

If a motor database with the rotor inertia and motor losses is available, these parameters can be added to the inverse kinetic model at this point of the motor selection process, instead of adding these parameters after selecting a motor, as proposed in Fig. 2. Automatic iterations can then be performed with this motor database to better select a motor without significant extra computational requirements. At each iteration loop, the torque vs. speed curve, calculated from the inverse kinetics that now includes the effect of the motor, will be compared to the motor torque vs. speed curve and evaluated, as described next to select a motor.

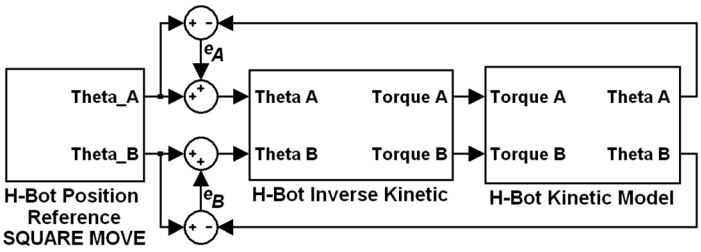

FIGURE 10. SIMULINK MODEL OF H-BOT AND CONTROL SYSTEM.

Torque vs. Speed Requirements

The open-loop simulation is used to determine the torque vs. speed requirement that each motor must develop for a given motion profile obtained from the worst case end-point trajectory. The selection of the appropriate motors for the simulated system relies on this estimated torque vs. speed curve.

The torque vs. speed curve of the H-Bot was obtained as follows. The position reference in Fig. 10 was calculated for a square move with a diagonal of 0.4m in Cartesian space to be completed in 2 seconds. The simulation of the H-Bot model, shown in this figure, yielded peak angular speeds between 440 and -440 rpm for both motors and peak torque of +0.91 to -0.22Nm for motor A and +0.22 to -0.91Nm for motor B. The torque and speed curves for motor A of the H-Bot are shown in Fig. 11.

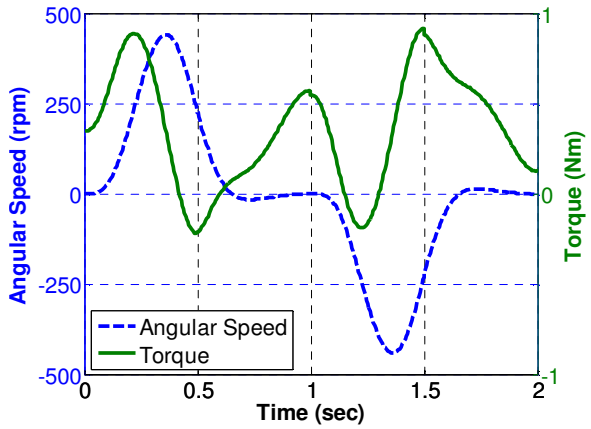

FIGURE 11. TORQUE AND SPEED PROFILE FOR MOTOR A OF THE SIMULATED H-BOT.

The data shown in Fig. 11 can then be plotted as a Torque vs. Speed curve, as shown in Fig. 12, which is the typical format to represent the data used to select motors. The torque vs. speed curves of the candidate motors must enclose the required torque vs. speed curve of the system. The other condition that needs to be satisfied is that the *rms* torque given at the *rms* speed of the application must be located below the continuous torque curve of the motor. Otherwise, the motor will overheat and potentially be damaged. The *rms* torque (τ_{rms}) and the *rms* speed (v_{rms}) are calculated as follows:

$$\tau_{rms} = \sqrt{\frac{1}{T}\int_0^T \tau^2(t)dt} \qquad (7)$$

$$v_{rms} = \sqrt{\frac{1}{T}\int_0^T v^2(t)dt}$$

τ is the instantaneous torque, v is the instantaneous velocity, and T is the total time of the data sample. The resulting *rms*

torque was calculated as 0.479 Nm at 206 rpm, as shown by the solid dot in Fig. 12 for this case-study robot.

Identifying candidate motors and choosing motors

The candidate motors (e.g., permanent-magnet synchronous motors, dc motors) are identified by comparing the required torque vs. speed curve and the *rms* torque at the *rms* speed with the torque vs. speed curve obtained from the motor datasheets. The candidate motors are those that enclose the required torque vs. speed curve. The inertia mismatch between the load and motor is, in general, preferred to be kept low (typically less than 10:1) to obtain higher system bandwidth. To keep the inertia ratio low, a gear box or a gearing mechanism may be necessary. Additional requirements, e.g., cost, voltage, energy efficiency, motor size and mounting orientation, will shorten the list of candidate motors. The manufacturers of the motors are, in general, limited to those that already supply parts to the machine builder.

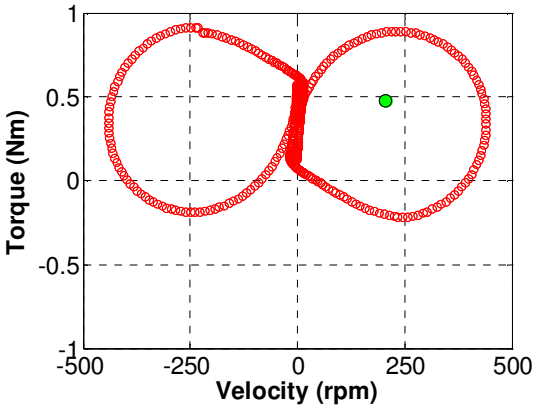

FIGURE 12. TORQUE AND SPEED PROFILE WITH RMS TORQUE AND RMS SPEED AT 3.79NM AND 20.5RPM.

The type of motor is also part of the motor selection. Torque density, rotor inertia, power, maximum speed, voltage, torque loses, frame type, operating temperature, are some of the characteristics that need to be taken into account while deciding for a particular motor technology.

Common types of motors used in industrial applications include induction motors, permanent magnet synchronous motors (PMSM), dc motors, and steppers [20]. Induction motors are used in general applications including pumps, conveyors, compressors, mixers, hoists, and cranes. This type of motor is low cost, robust, easy to maintain, and is available from fractions to hundreds of a horse-power. They can either be powered directly from the power line, as well as via variable frequency drives (VFD). When powered via VFDs, motors can be controlled from nearly zero to the rated speed and develop rated torque in this speed range, which is not possible when powered directly from the power line. Permanent magnet synchronous motors (PMSM) can have low rotor inertia and high torque density, which make them suitable for motion control applications, where fast transitions in speed and positioning accuracy are required. Typical applications for PMSM motors include packaging machines, web handling, cartoners, fillers, robots, and capping machines. DC motors are relatively easy to model and can have simple speed control methods and develop high torque [20, 21]. This allows this type of motor to be used in a variety of applications, including power tools, mining equipment, and robots. The stepper motors are commanded in incremental steps. Each step yields a fixed angular displacement which can be in the forward or reverse direction. As long as no steps are missed, there is a synchronous relationship between the input command and the angular position of the motor shaft, which can yield an accurate open-loop positioning system. Thus, typical applications for stepper motors include printers, disk drives, and machine tools.

Since the control of an H-Bot characterizes a motion-control application, a PMSM was chosen as the motor type. By comparing the curve in Fig. 12 for motor A of the H-Bot with a variety of torque vs. speed curves of PMSM motors, the motor shown in Table 1 was selected in conjunction with a 10:1 gear box. The same analysis was repeated for motor B of the H-Bot and the same motor and gearbox were selected. If an electronic database of the motors under consideration is available, this selection process can be automated.

TABLE 1. SELECTED MOTOR FOR THE H-BOT

	Parameter	Unit
Voltage	460	Vac
Continuous Torque	0.26	Nm
Peak Speed	8000	rpm
Rotor Inertia	7.41×10^{-6}	kg-m^2
Torque Constant	0.3	Nm/A
Part Number	MPL-B1510V	-
Manufacturer	Allen-Bradley	-

Augmenting the system

The chosen motor becomes an integral part of the system, and its properties, including rotor inertia and torque losses, must be included in the model of the system. Any flexible couplings or gearing contained in the system should also be included in the model. If a gearbox or a transmission mechanism is added to the system to reduce the inertia ratio between the load and motor or increase available torque, not only the gear ratio, but also the losses and inertia of this additional component, must be included in the system.

Control System Design

A typical control scheme for motor control consists of a cascaded control with an inner velocity PI (Proportional-Integral)

control and an outer position PI control, as shown in Fig. 13. A feedforward velocity loop (FFv) is used to reduce position-following error, while the acceleration feedforward loop (FFa) can be used to reduce velocity-following error. The velocity loop feeds the current loop that controls the energy delivered to the motor to move according to the commanded position profile and feedback response. Two filters were placed between the velocity and current loops to be used as needed: a low pass filter (LPF) to reduce high frequency noise feeding the current loop and a notch filter (NF) to reduce the effect of resonant frequencies.

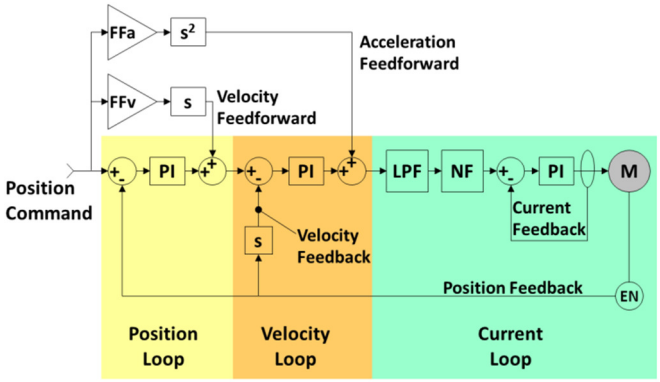

FIGURE 13. CASCADE PI CONTROL FOR ONE OF THE H-BOT MOTORS.

Tuning

The tuning process must start with the PI gains of the position and velocity loops to make the system robust to load disturbances. Then, the velocity feedforward and acceleration feedforward gains can be used to reduce tracking errors.

Closed-Loop Simulation

In the closed-loop simulation, the motion position profile defined via trajectory planning and inverse kinematics is applied to the cascade control that closes the loop with the kinetic model of the system. The cascade control consists of the position and velocity loops shown in Fig. 13. The resulting motion profile from the kinetic model can be compared to the reference signal from the motion profile command to evaluate the position-following error. This closed-loop simulation is used to verify if the system requirements are met. The closed-loop model for the H-Bot is shown in Fig. 14.

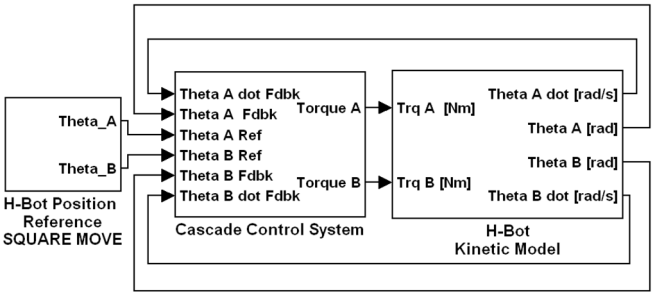

FIGURE 14. CLOSED-LOOP MODEL OF THE H-BOT.

Final torque vs. speed requirements and possible iterations

If the following requirements are met, the selected motor is a valid solution:

- torque vs. speed curve of the system (including gearbox or transmission, if any) still resides within the torque vs. speed curve of the motor after including the rotor inertia and motor losses and tuning the closed-loop system,
- the *rms* torque and *rms* speed are still under the continuous torque curve of the gear-motor, and
- the system develops a stable response.

If some of these requirements are not met with the selected motor, iterations are needed, i.e., different motors and/or gear boxes need to be evaluated until a valid solution is found. However, in applications where the torque vs. speed requirement is too high, a valid motor/gear box solution may not exist. In this case, the mechanism or the application requirements need to be reevaluated.

SIMULATION RESULTS

The simulation results of the proposed motor selection process and the trajectory planning are presented next.

Motor selection process validation

The motor inertia defined in Table 1 and the 10:1 gear ratio of the gear box was added to the kinetic model of the H-Bot shown in Fig. 9. After tuning the cascade position and velocity control system, shown in Fig. 13, for each motor, the complete closed-loop system, shown in Fig. 14, was simulated.

The torque vs. speed curve obtained from the tuned closed-loop system for the square move of a 0.4 m diagonal in 2 seconds is shown in Fig. 15. By comparing the open-loop torque vs. speed curve shown in Fig. 12 with the closed-loop torque vs. speed curve shown in Fig. 15, good agreement was obtained. The open-loop simulation yielded peak torque from +0.91 to -0.22 Nm while the closed-loop simulation yielded peak torque from +1.04 to -0.34 Nm for motor A. This difference is mainly due to the extra load caused by the inertia of the motor and gear box added to the closed-loop system and to the extra torque commanded by the cascade control system to yield low position following error.

Trajectory planning validation

In order to demonstrate the gain in positioning accuracy with the trajectory planning approach presented in this paper, a comparison between the traditional and the proposed trajectory planning was performed. The traditional trajectory planning here consists of a master reference running at constant speed, which yields the motion profile command shown in Fig. 6. The results of this comparison are shown in Fig. 16. The position error obtained with the proposed trajectory planning was 0.5 mm, which is within the 1 mm maximum error from the system requirements. However, when the position commands (θ_A and θ_B)

applied to the motors were calculated with the traditional trajectory planning, the position error increased to 3.3 mm which is higher than the system requirements. In addition, to meet the position error requirement, the presented trajectory planning yielded an end-point trajectory profile closer to a square shape than the profile obtained with the traditional trajectory planning. It can be observed from Fig. 16 that the accuracy to trace the corners with the proposed trajectory planning was improved by simply shaping the profile of the command reference (θ_A and θ_B) applied to the motor for the same end-point trajectory executed in the same amount of time. Consequently, lower product imperfections would occur. The tuning of the control system was kept exactly the same for this test.

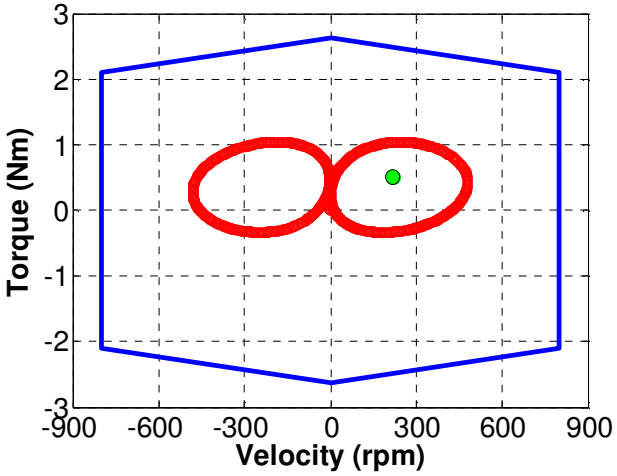

FIGURE 15. TORQUE VS. SPEED CURVE OF THE H-BOT OBTAINED FROM THE CLOSED-LOOP SIMULATION. THE EXTERNAL CURVE IS THE CONTINUOUS TORQUE VS. SPEED CURVE OF THE SELECTED MOTOR.

When the traditional and proposed trajectory planning are compared in terms of torque profile applied to the motors, the traditional method yielded peak-to-peak torque of 12.46 Nm, while the presented method yielded peak-to-peak torque of 1.38 Nm (Figure 17). Thus, the traditional method yielded a peak-to-peak torque nine times higher than the presented method. These large peak torques have higher jerk content than the torque profile obtained with the presented trajectory planning. These peak torques can possibly cause mechanical vibrations, stress on mechanical and electronic components, electrical and audible noise, and stress on motors and actuators.

Thus, a systematic motor selection process associated with an appropriate trajectory planning method helps to obtain a stable system with low jerk content and accurate positioning throughout the end-point trajectory, including the corners.

The parameters of the H-Bot used to obtain the results presented in this paper are shown in Table 2.

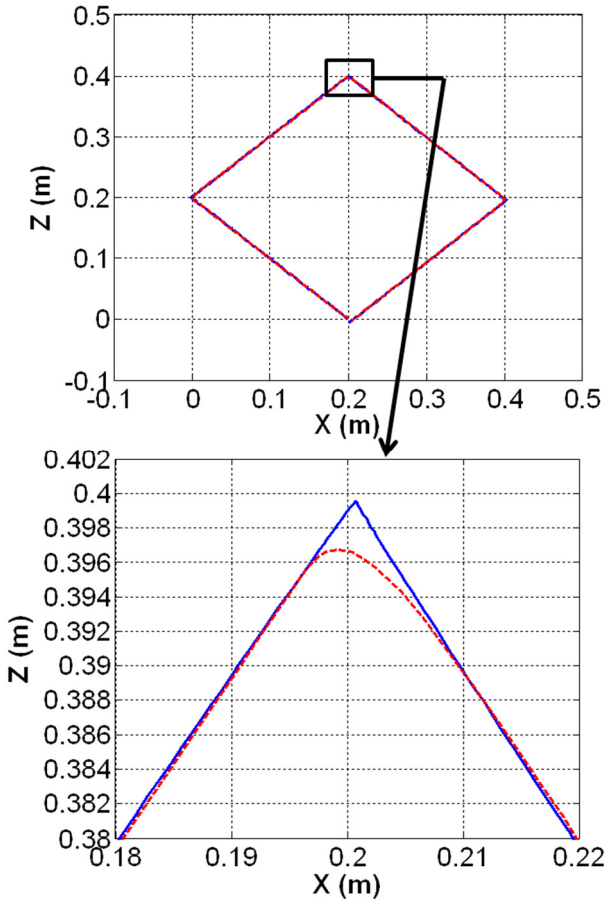

FIGURE 16. COMPARISON BETWEEN THE POSITIONING ACCURACY OBTAINED WITH TRADITIONAL (DASHED LINE) AND PROPOSED (SOLID LINE) TRAJECTORY PLANNING FOR THE H-BOT.

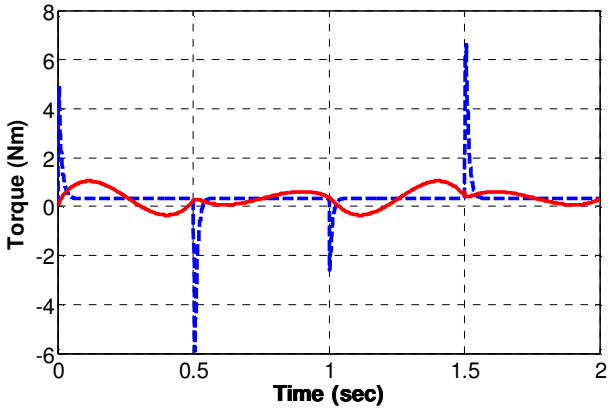

FIGURE 17. COMPARISON BETWEEN TORQUE FOR MOTOR A WHEN USING PROPOSED (SOLID LINE) AND TRADITIONAL (DASHED LINE) TRAJECTORY PLANNING.

TABLE 2. H-BOT PARAMETERS

	Parameter	Unit
Radius of the pulleys (r)	0.03	m
Vertical moving mass (m_1)	2.4	kg
Horizontal moving mass (m_2)	3.9	kg
Pulley Inertia (I_A and I_B)	3.1×10^{-4}	kg-m^2

CONCLUSIONS

Some of the challenges in the design of high-performance machines reside in the appropriate selection of motors and the calculation of the position reference for these axes. A model-based design approach to properly select a motor, and a trajectory-planning method to calculate the position command to the motors were proposed in this paper to address these challenges. This approach can be used in the motor selection process for industrial machines used in a variety of applications including packaging, metal-forming, converting, assembly, material handling, and robotics. This proposed motor selection process was demonstrated by selecting the motors for both axes of a planar robot called an H-Bot. The trajectory planning method presented here was used to calculate the position reference for the axes of an H-Bot to perform a square path. The resulting motion profile from this trajectory planning helps mitigate the effects of vibration, stress to mechanical and electronic systems, electrical and audible noise, as well as to improve the performance of the system by reducing position-following error. A traditional and the presented trajectory planning approaches were used to command the motion of the H-Bot and the results were compared. The position-following error obtained with the presented trajectory planning was within the system requirements, while the position error obtained with the traditional trajectory planning was over three times higher than the requirements. Additionally, the peak torques with the traditional trajectory planning method were nine times higher than the presented trajectory planning method.

REFERENCES

[1] SolidWorks. Incorporating Mechatronics into Your Design Process. [White Paper].

[2] K. Perrin, "Enabling Mechatronics Product Development with Digital Prototyping," ed. Autodesk Website: Autodesk, 2008.

[3] R. Isermann, "Modeling and Design Methodology for Mechatronic Systems," *IEEE/ASME Transactions on Mechatronics,* vol. 1, p. 13, March, 1996 1996.

[4] H. Arioui, *et al.*, "Mechatronics, Design, and Modeling of a Motorcycle Riding Simulator," *IEEE/ASME Transactions on Mechatronics,* vol. 15, pp. 805-818, 2010.

[5] GM. (2009), GM Standardizes on Model-Based Design for Hybrid Powertrain Development. [User Story]. 1-2. Available: http://www.mathworks

[6] Z. Yong, *et al.*, "Mechatronic Modeling and Analyzing for Feed Servo Control System Based on Torsion Dynamics of Lead-Screw," in *2010 International Conference on Measuring Technology and Mechatronics Automation (ICMTMA)*, 2010, pp. 632-635.

[7] Xerox. (2004), Xerox Reduces Development Time Using MathWorks Tools. [User Story]. 1-2. Available: http://www.mathworks.com

[8] Segway. (2003), Segway LLC Delivers Innovative Transporter Using MathWorks Tools. 1-2. Available: http://www.mathworks.com

[9] S. Macfarlane and E. A. Croft, "Jerk-bounded manipulator trajectory planning: design for real-time applications," *IEEE Transactions on Robotics and Automation,* vol. 19, pp. 42-52, 2003.

[10] H. Ming-Shyan, *et al.*, "Minimum-Energy Point-to-Point Trajectory Planning for a Motor-Toggle Servomechanism," *IEEE/ASME Transactions on Mechatronics,* vol. 17, pp. 337-344, 2012.

[11] H. Panfeng, *et al.*, "Motion Trajectory Planning of Space Manipulator for Joint Jerk Minimization," in *International Conference on Mechatronics and Automation*, 2007, pp. 3543-3548.

[12] Y. Guan, *et al.*, "On robotic trajectory planning using polynomial interpolations," in *IEEE International Conference on Robotics and Biomimetics*, 2005, pp. 111-116.

[13] I. H. Liu, *et al.*, "Planning and implementation of motion trajectory based on C2 PH spline," in *IECON 2011 - 37th Annual Conference on IEEE Industrial Electronics Society*, 2011, pp. 246-251.

[14] C. H. Moon, "Cam Design," ed. Wheeling, IL: Commercial Cam Division, Emerson Electric Company, 1961, p. 69.

[15] R. L. Norton, *Cam Design and Manufacturing Handbook*, 2nd ed. New York: Industrial Press, Inc., 2009.

[16] G. K. Singh and J. Claassens, "An analytical solution for the inverse kinematics of a redundant 7DoF Manipulator with link offsets," in *IEEE/RSJ International Conference on Intelligent Robots and Systems (IROS)*, 2010, pp. 2976-2982.

[17] S. Parasuraman, *et al.*, "Trajectory planning for redundant manipulator using evolutionary computation technique," in *IEEE Instrumentation and Measurement Technology Conference (I2MTC)*, 2011, pp. 1-6.

[18] G. D. Wood and D. C. Kennedy. (2003, Simulating Mechanical Systems in Simulink with SimMechanics. 1-25. Available:

[19] J. Ginsberg, *Engineering Dynamics*. New York: Cambrige University Press, 2008.

[20] A. E. Fitzgerald, *et al.*, *Electric Machinery*, 6th ed.: McGraw-Hill, 2002.

[21] C. W. d. Silva, *Mechatronics: A Foundation Course*. New York: CRC Press, 2010.